
















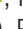
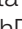



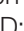









ORIGINAL RESEARCH

Vessel-Specific Myocardial Mass in Patients With Stable Coronary Artery Disease

Nikolaos Stalikas , MD, PhD; Takuya Mizukami, MD, PhD; Frederic Bouisset , MD; Kazumasa Ikeda , MD; Atomu Tajima, MD; Daniel Munhoz , MD, PhD; Thabo Mahendiran, BMBCh, MD; Adriaan Wilgenhof, MD; Koshiro Sakai , MD, PhD; Bjarne Noorgard , MD, PhD; Thomas Engstroem , MD; Jonathon Leipsic , MD; Giulio Stefanini , MD, PhD; Antonio Bartorelli, MD; Timothy Fairbairn , MD; Alan Bagnall , MD, PhD; Brian Ko , MD, PhD; Nils P Johnson , MD; Colin Berry , MD, PhD; Divaka Perera , MD, PhD; Evald Høj Christiansen , MD; Toshiro Shinke , MD, PhD; Hiromase Otake , MD, PhD; Bon Kwon Koo , MD, PhD; Emanuele Barbato , MD, PhD; Salvatore Brugaletta , MD; Damien Collison , MD; Gianluca Campo , MD; Eric Van Belle , MD, PhD; Tommaso Goori, MD, PhD; Lokien Van Nunen , MD; Adam Witkowski , MD, PhD; Patricio Astudillo, PhD; James Spratt , MD; Tetsuya Amano , MD, PhD; Hirohiko Ando , MD, PhD; Georgios Sianos , MD, PhD; Jeroen Sonck , MD, PhD; Daniele Andreini, MD, PhD; Bernard De Bruyne , MD, PhD; Carlos Collet , MD, PhD

BACKGROUND: Assessing the myocardial mass at risk is essential in evaluating patients with coronary artery disease. This study aims to establish reference values for vessel-specific myocardial mass derived from coronary computed tomography angiography, providing a quantitative assessment of the myocardial mass subtended by each epicardial vessel.

METHODS: Left ventricular (LV) and vessel-specific myocardial mass were calculated from coronary computed tomography angiography using the Voronoi method in patients with stable coronary artery disease. Myocardial mass was quantified for each epicardial coronary artery with a diameter >1.5 mm.

RESULTS: We included 948 patients with 9228 epicardial coronary artery branches. Mean age was 66 ± 9 years. The cohort was predominantly male (77%); 66% had hypertension, and 22% had diabetes. Vessel-specific myocardial mass was calculated for 2767 main epicardial arteries (948 left anterior descending, 948 left circumflex, and 871 right coronary artery) and 6461 side branches (1888 diagonals, 1208 septals, 1422 obtuse marginals, 247 ramus intermedius, 850 right posterior descending, and 846 posterolateral branches). Median LV mass was 141 grams (interquartile range 118–166); women had smaller LV mass than men (106 [93–123] grams versus 150 [132–173] grams, $P < 0.001$). On average, the left anterior descending subtended 42.5% [37.9–48.1] of LV mass, the left circumflex artery 28.8% [21.9–5.7], and the right coronary artery 26.4% [20.9–31.9]. Median LV mass subtended by the first septal, first diagonal, and first obtuse marginal were 8.9% [6.4–11.1], 7.9% [4.52–2.0], and 10.2% [4.52–12.0], respectively.

CONCLUSIONS: This study quantified the myocardial mass subtended by each major artery in the coronary circulation. Understanding the vessel-specific mass at risk has significant clinical implications for personalizing revascularization strategies.

REGISTRATION: This is a retrospective analysis of 5 prospectively conducted trials (P3: NCT03782688; P4: NCT05253677; PPG Global: NCT04789317; Euro-CRAFT: NCT05805462; INSIGHTFUL-FFR: NCT05437900). No additional registration was required.

Key Words: coronary artery disease ■ coronary CT angiography ■ myocardial mass ■ vessel-specific analysis

See Editorial by XXX

Correspondence to: Carlos Collet, MD, PhD, Cardiovascular Center Aalst, OLV-Clinic, Moorselbaan, 1654, Aalst B-9300, Belgium. Email: carloscollet@gmail.com

This article was sent to Nadia R. Sutton, MD, MPH, Associate Editor, for review by expert referees, editorial decision, and final disposition.

Supplemental Material is available at <https://www.ahajournals.org/doi/suppl/10.1161/JAHA.124.039013>

For Sources of Funding and Disclosures, see page 9.

© 2025 The Author(s). Published on behalf of the American Heart Association, Inc., by Wiley. This is an open access article under the terms of the [Creative Commons Attribution-NonCommercial-NoDerivs](#) License, which permits use and distribution in any medium, provided the original work is properly cited, the use is non-commercial and no modifications or adaptations are made.

JAHA is available at: www.ahajournals.org/journal/jaha

CLINICAL PERSPECTIVE

What Is New?

- This study introduces a novel approach to automatically quantify vessel-specific myocardial mass using coronary computed tomography angiography and provides reference ranges for left ventricular mass subtended by each epicardial vessel, enhancing understanding of myocardial distribution and improving risk assessment in coronary artery disease.

What Are the Clinical Implications?

- Integrating vessel-specific myocardial mass quantification into routine coronary computed tomography angiography could enhance personalized care for patients with stable coronary artery disease.
- This method could improve revascularization planning by offering precise data on myocardial territories at risk, particularly in cases involving bifurcation or intermediate lesions, ultimately improving patient outcomes through tailored therapeutic strategies.

Nonstandard Abbreviations and Acronyms

OM	obtuse marginal
PDA	posterior descending artery

Myocardial mass at risk in patients with coronary artery disease (CAD) is a well-established predictor of prognosis.¹ In patients who experience a myocardial infarction, the affected mass associates directly with heart failure and cardiac death.^{2,3} Additionally, in patients considered for revascularization, evaluating the myocardial mass at risk is a key element of the decision-making process.⁴

Left ventricular (LV) myocardial mass can be quantified using various imaging modalities, including echocardiography, cardiac magnetic resonance imaging, nuclear perfusion scans, and coronary computed tomography angiography (CCTA).^{5,6} CCTA uniquely allows for direct measurements of myocardial mass subtended by each coronary artery using 2 methods. The Voronoi method subdivides the LV myocardium using a nearest-neighbor assignment to the subtending vessel.⁷ Another method applies allometric scaling laws, using diameter-derived regional flow as a proportion of the myocardial volume.⁸

Although quantification of myocardial mass at risk is not routinely performed using CCTA, it may

provide valuable data for clinical decision-making. Consequently, assessing the myocardial mass subtended by each coronary artery is important. This study aims to establish reference values for vessel-specific myocardial mass derived from CCTA.

METHODS

Data Availability Statement

The data that support the findings of this study are available from the corresponding author (Dr Carlos Collet) upon reasonable request. Due to privacy regulations, some restrictions may apply. No analytic code was used beyond standard R functions and packages (R version 4.0.2).

Study Design

This is a pooled analysis of 5 prospective studies (P3 [Precise Percutaneous Coronary Intervention Plan] Study, NCT03782688; P4 [Precise Procedural and PCI (Percutaneous Coronary Intervention) Plan], NCT05253677; PPG Global [Pullback Pressure Gradient Global Registry], NCT04789317; The Euro-CRAFT Registry [European Microcirculatory Resistance and Absolute Flow Team], NCT05805462; and INSIGHTFUL-FFR [Pressure Microcatheter Vs Pressure Wire For Decision Making Randomized Clinical Trial] NCT05437900) conducted at 32 sites involving stable patients with CAD. Study design and inclusion and exclusion criteria are shown in [Tables S1](#) and [S2](#). Patients with prior coronary artery bypass grafting, ST-segment-elevation myocardial infarction, severely reduced LV ejection fraction (<30%), or poor CCTA image quality were excluded. Chronic total occlusion was also an exclusion criterion in 4/5 studies included (P3 Study, PPG Global, Euro-CRAFT, and INSIGHTFUL-FFR) ([Figure S1](#)). CCTA analyses were performed by a Core Laboratory (CoreAalst BV, Aalst, Belgium). Race was assigned based country of inclusion, and hypertension and diabetes were defined according to clinical history or the use of antihypertensive and antidiabetic medications, respectively. Local ethics committees approved the original study protocols, and all patients provided written informed consent.

Myocardial Mass Measurement

CCTA scans were acquired using various CT scanners ([Table S3](#)). CCTA was performed according to the Society of Cardiac Computed Tomography recommendations, including nitrates and beta-blockers before image acquisition.⁹ Whole LV and vessel-specific LV mass were automatically calculated using dedicated software (Synapse Vincent ver.5; Fujifilm Medical Systems, Tokyo, Japan). After automatic LV

segmentation, the software employed the Voronoi algorithm to subdivide the LV myocardium according to the subtending arteries. CCTA-derived vessel-specific myocardial mass based on the Voronoi algorithm has been histologically validated and is substantially correlated with actual vessel-specific myocardial mass measured on ex vivo swine hearts.¹⁰ This subdivision is based on a nearest-neighbor computation, using principles of the Voronoi diagram to divide the LV into distinct regions, each associated with a single generating point (or seed).¹¹ The algorithm assigns each voxel of the LV volume to the nearest voxel of an adjacent coronary artery, effectively connecting each myocardial region to its closest coronary artery. Once this connection is established, the algorithm aggregates all myocardial voxels associated with the voxels of the coronary artery distal to the seed point. This aggregation allows for automatic calculation of the LV volume subtended by each coronary artery. Subsequently, the LV mass is calculated by multiplying the aggregated volume of these myocardial voxels by a constant factor of 1.05 g/cm³ representing the density of myocardial tissue.¹² The software recognizes all side branches with a diameter >1.5 mm. The software automatically calculates the subtended LV mass for the left anterior descending (LAD), left circumflex (LCX), and right coronary artery (RCA). To calculate the mass subtended by each vessel, a seed point was placed at the ostium of the vessel (Movie S1 and corresponding still image Figure S2). Coronary dominance was defined by the presence of the posterior descending artery (PDA). Myocardial mass supplied by the PDA included the regions served by all side branches running in the posterior interventricular groove distal to the crux. Similarly, the mass supplied by the posterolateral branch encompassed the LV mass served by all side branches originating from the distal right coronary artery from the crux. In cases of left coronary dominance, the mass supplied by the PDA included the most distal side branch of the dominant LCX.¹³

Statistical Analysis

Descriptive statistics were calculated for both continuous and categorical variables. Continuous variables were summarized using means, SDs, medians, interquartile ranges, and ranges depending on the distribution of the variable. Categorical variables were analyzed by computing frequencies and percentages, then displayed in contingency tables. Independent *t* tests were used to compare LV mass between binary categorical groups, including sex, race, body mass index (BMI) categories, and hypertension status. ANOVA was performed to compare LV mass among groups categorized by coronary dominance and anatomical variation, followed by Tukey's post hoc tests when ANOVA was

significant. Violin plots illustrating the distribution and probability density of vessel-specific LV mass by coronary dominance have also been described accordingly. Correlation analyses (Pearson's correlation coefficient) were performed to evaluate relationships between LV mass, age and BMI.

Finally, univariate and multivariable regression analyses were conducted to identify predictors of LV mass (including age, sex, race, BMI, diabetes, hypertension, and dyslipidemia). Given the descriptive primary aim of this study, detailed results of these analyses are provided in Table S4. A *P* value of <0.05 was considered statistically significant. All analyses were performed using R version 4.0.2 (R Core Team, 2020).

RESULTS

In total, 948 patients with 9228 epicardial coronary artery branches were included. The mean age was 66±9 years. The cohort was predominantly male (77%), with 66% having hypertension and 22% diabetes. Baseline clinical characteristics are shown in Table 1. A total of 2767 main coronary vessels (LAD 948, LCX

Table 1. Baseline Characteristics

	Overall (N=889)
Age, y, mean±SD	65.6 (9.2)
Body mass index, kg/m ² , mean±SD	26.5 (3.8)
Female sex, n (%)	206 (23.2)
Hypertension, n (%)	586 (66.0)
Diabetes, n (%)	192 (21.7)
Dyslipidemia, n (%)	740 (83.4)
Smoking, n (%)	175 (19.7)
CAD*, n (%)	419 (96.5)
Prior percutaneous coronary intervention, n (%)	28 (3.1)
Prior myocardial infarction, n (%)	20 (2.2)
Peripheral artery disease, n (%)	37 (4.2)
Race†, n (%)	
White, n (%)	463 (69.7)
Asian, n (%)	202 (30.3)
Clinical presentation	
Asymptomatic, n (%)	35 (4.0)
Silent ischemia, n (%)	68 (7.6)
Stable angina, n (%)	773 (87.0)
Unstable angina, n (%)	9 (1.0)
Non-ST-segment-elevation myocardial infarction, n (%)	4 (0.4)

Baseline characteristics are available in 889 out of 949 patients who underwent CCTA.

*Available data in 419 patients. Obstructive CAD was defined based on visual assessment of diameter stenosis ≥50% in at least one main coronary artery.

†Available data in 665 out of 949 patients who underwent CCTA. CAD, coronary artery disease.

948, and RCA 871) and 6461 side branches (diagonals 1888, septals 1208, obtuse marginal [OM] 1422, ramus intermedius 247, PDA 850, and posterolateral branch 846) underwent measurement of the subtended LV mass (Table 2).

Median LV mass was 141 grams (interquartile range, 118–166). There was a weak but significant negative correlation between LV mass and age ($r = -0.20$ [95% CI, -0.26 to -0.14], $P < 0.001$; Figure 1). Patients >65 years had less myocardial mass compared with younger patients (135 grams [110–160] versus 149 grams [126–173], $P = 0.001$). Likewise, women had less LV mass compared with men (106 grams [93–123] versus 150 grams [132–173], $P < 0.001$). Additionally, Asian patients had lower myocardial mass than White patients (130 grams [104–155] versus 144 grams [119–167], $P = 0.05$) (Table S5). There was a weak but significant positive correlation between LV mass and BMI ($r = 0.32$ [95% CI, 0.26 – 0.37], $P < 0.001$). Patients with a BMI ≥ 25 kg/m² had significantly greater LV mass compared with those with a BMI < 25 kg/m² (149 grams [125–174] versus 127

grams [106–150], $P < 0.001$, Figure S3). Patients with hypertension exhibited greater LV mass than patients without hypertension (143 grams [119–169] versus 138 grams [111–159], $P = 0.01$). Univariate and multivariable regression analyses for the association between LV and clinical characteristics are shown in Figure S4.

Vessel-Specific Myocardial Mass

Median LV mass supplied by the LAD was 59 grams [47–74], by the LCX 40 grams [27–56], and by the RCA 37 grams [27–47]. Accordingly, the LAD subtended 42.5% [37.9–48.1] of the LV mass, and the LCX and RCA subtended 28.8% [21.9–35.7] and 26.4% [20.9–31.9] of the LV mass, respectively (Figure 2).

Median LV mass subtended by the first septal, first diagonal, and first OM artery were 12 grams [8–17], 11 grams [6–18], and 14 grams [7–23], respectively. The first septal subtended 8.9% [6.4–11.1], the first diagonal 7.9% [4.5–12.0], and the first OM subtended 10.2% [5.1–17.0] of the LV mass (Figure 3). The second OM subtended 10.1% [5.5–15.7] of the LV mass.

Table 2. Distribution of Vessel-Specific LV Mass

	No.	Subtended LV mass (g)	Percentage of LV mass (%)
LV	948	141 (118–166)	
Left dominance	103	147 (125–167)	
Right dominance	845	140 (116–166)	
LAD	948	59 (47–74)	42.5 (37.9–48.1)
LCX	948	40 (27–56)	28.8 (21.9–35.7)
RCA*	871	37 (27–47)	26.4 (20.9–31.9)
Ramus intermedius	246	15 (7–26)	10.0 (5.0–17.7)
Diagonals	1888		
Diagonal 1	893	11 (6–18)	7.9 (4.5–12.0)
Diagonal 2	663	9 (5–14)	6.3 (3.5–9.7)
Diagonal 3	285	5 (3–9)	3.7 (2.3–6.2)
Diagonal 4	44	5 (3–7)	2.8 (2.1–5.5)
Diagonal 5	3	2 (2–4)	1.6 (1.3–1.9)
Septals	1208		
Septal 1	800	12 (8–17)	8.9 (6.4–11.1)
Septal 2	331	5 (3–9)	3.7 (1.9–6.1)
Septal 3	65	4 (2–6)	2.9 (1.7–4.5)
Septal 4	11	5 (3–6)	3.2 (2.5–4.7)
Septal 5	1	4 (4–4)	4.5 (4.5–4.5)
OM	1422		
OM1	820	14 (7–23)	10.2 (5.1–17.0)
OM2	454	13 (7–22)	10.1 (5.5–15.7)
OM3	135	13 (9–20)	9.5 (6.0–14.0)
OM4	13	11 (9–17)	6.4 (5.4–11.3)
Posterolateral branch	846	16 (10–23)	11.3 (7.8–15.7)
Posterior descending artery	850	18 (13–24)	13.0 (10.0–16.3)

Values are presented as Median (IQR). LAD indicates left anterior descending; LCX, left circumflex; LV, left ventricle; OM, obtuse marginal; and RCA, right coronary artery.

*RCA did not subtend any part of LV mass in 77 out of 103 patients with left dominance.

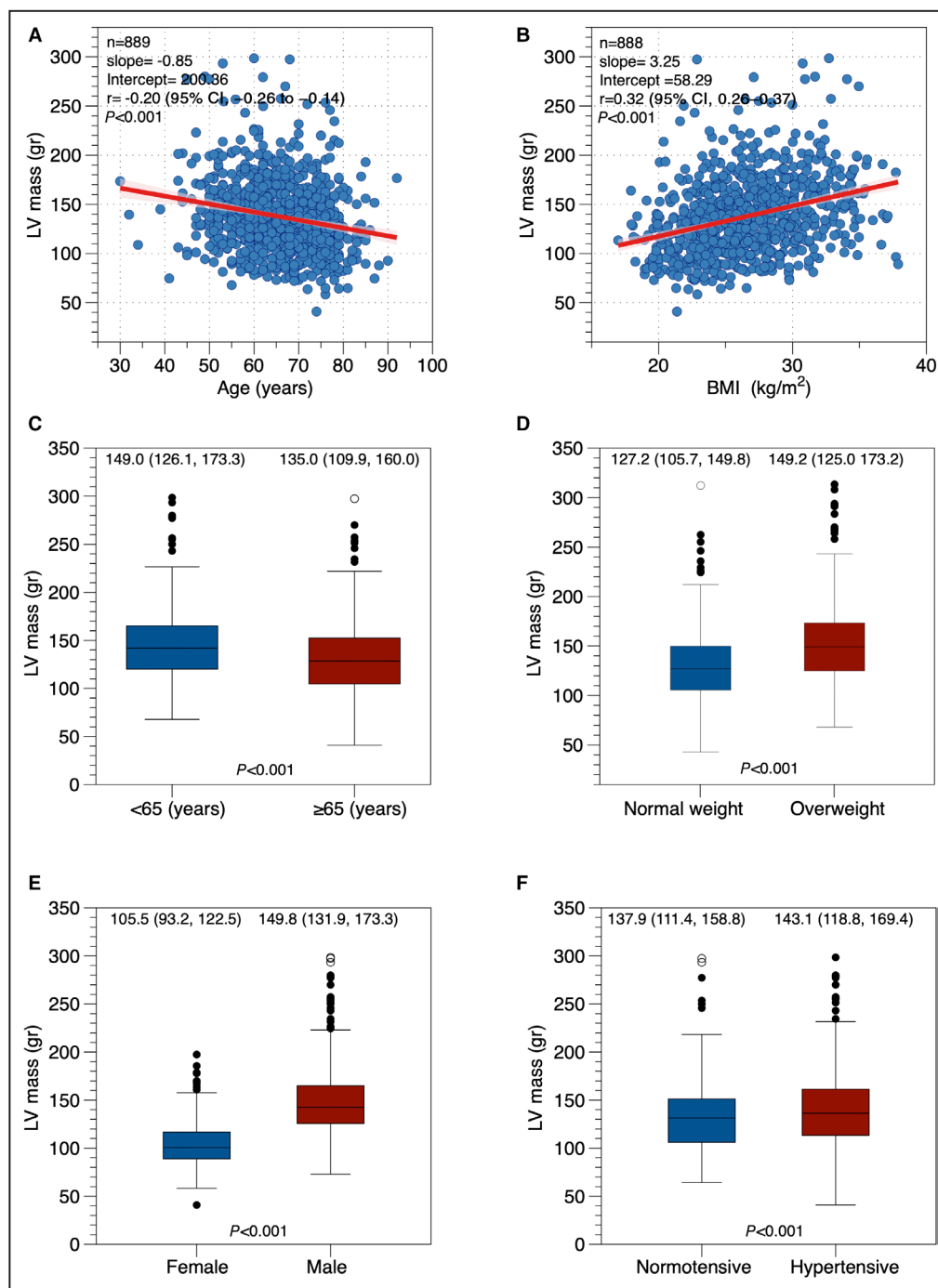


Figure 1. Comparison of myocardial mass in different groups.

A, Correlation between LV mass and age. **B**, Correlation between LV mass and BMI. **C–F**: Boxplots comparing LV mass across categorical groups. The numbers above each boxplot represent the median LV mass and interquartile range (Q1–Q3). **C**, Comparison of LV mass between individuals aged <65 and those aged ≥65. **D**, Comparison of LV mass between normal weight (BMI<25) and overweight (BMI≥25) patients. **E**, LV mass according to sex. **F**, Comparison of LV mass based on hypertension status. BMI indicates body mass index; and LV, left ventricular.

Myocardial Mass in Patients With Left Dominant Circulation

Left dominance was observed in 11% (103 patients) of the total population. Patients with a left dominant

coronary circulation exhibited a significantly greater mass subtended by the LCX compared with those with right dominance (47.5% [39.4–52.6] versus 27.7% [21.0–33.7], $P < 0.001$, Figure 4). Notably, in patients with a left dominant circulation, the LCX subtended a similar

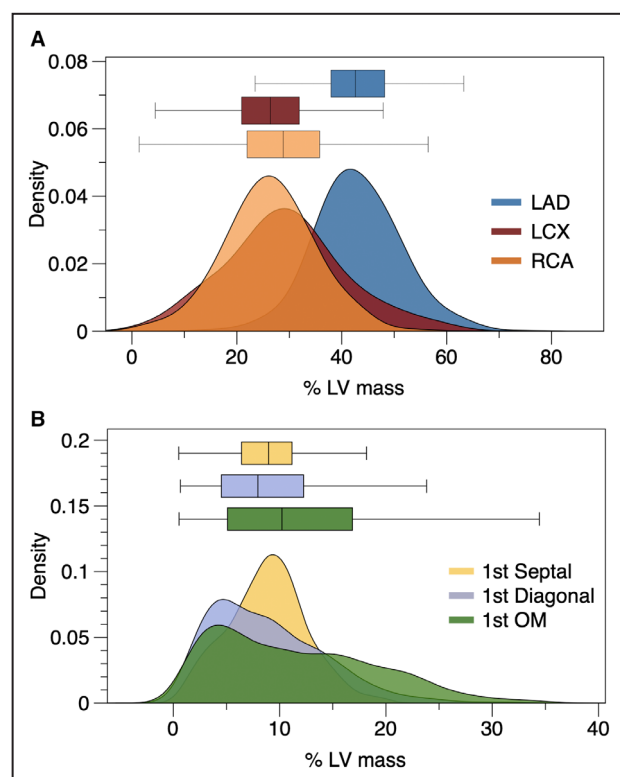


Figure 2. Distribution of left ventricular mass subtended by major coronary arteries and branches.

A. The density plots display the percentage of LV mass subtended by the LAD, LCX, and RCA. The x axis represents the percentage of LV mass, and the y axis represents the density of the distribution. The overlapping regions indicate the distribution of LV mass shared among these vessels, highlighting the LAD having the highest density peak around 50%. The RCA and LCX have their peaks around 20% and 30% respectively. **B.** The density plots reveal that the first septal branch has a peak density at around 10%. The first diagonal and first OM branches show a broader distribution, with their peaks around 10% and 15%, respectively. LAD indicates left anterior descending; LCX, left circumflex; LV, left ventricular; OM, obtuse marginal; and RCA, right coronary artery.

percentage of the LV mass as the LAD (47.5% [39.4–52.6] versus 46.4% [41.6–50.9], $P=0.78$, Table S6). Furthermore, in cases with left dominance, the LAD subtended a greater myocardial mass than in cases with right dominance (46.5% [41.6–50.9] versus 42.2% [37.6–47.6], $P<0.001$).

Myocardial Mass in Patients With Left Main Trifurcation

In 27% of the cases (246 patients), left main trifurcation anatomy was observed. In these cases, the LCX subtended a smaller portion of the LV mass compared with those with a left main bifurcation (30.4% [24.4–36.5] versus 34.6% [28.1–40.2], $P<0.001$). Median mass subtended by the ramus intermedius artery was 15 grams [7–26], which represented 10.1% [5.1–17.8] of the LV mass.

Side Branches Subtending >10% LV Mass

Among diagonals, marginals, PDA, and posterolateral branch ($n=5006$), 2475 (49%) subtended more than 10% of the LV mass. Specifically, 35.6% of first diagonals, 50.4% of first OMs, and 50.9% of second OM branches subtended more than 10% of the LV mass (Figure S5). In patients with only 1 diagonal branch, the median mass subtended by the diagonal was 12.2% [8.8–15.6], and in 62% of these cases, it subtended more than 10% of the LV mass. In cases with >1 diagonal, the median mass subtended by the first diagonal was 6.5% [4.0–9.9], and in 23% of cases subtended >10% of the LV mass (Figure S6). In cases with a single OM branch, the median subtended LV mass was 15.6% [8.8–20.9], and in 66% of cases it subtended >10% of the LV mass. In cases with >1 OM, the median mass subtended by the first OM was 7.1% [3.6–11.8], and in 27% of cases, it subtended >10% of the LV mass.

Septal branches subtended a median of 10.2% [6.6–12.9] of the LV, and 38% of first septals subtended >10% of the LV mass. In cases with a single septal branch, the median subtended LV mass was 9.4% [7.4–11.5], and 42% subtended >10% of the LV mass. In cases with multiple septal branches, the median mass subtended by the first septal was 8.0% [4.5–10.3], and in 21% of cases it subtended >10% of the LV mass.

DISCUSSION

To our knowledge, this study is the largest analysis describing the distribution of myocardial mass subtended by each coronary artery and provides reference values for clinical use. Additionally, we observed sex and racial differences in LV mass, as well as a decline in LV mass with age. Furthermore, patients with arterial hypertension and obesity exhibited a greater LV mass. When examining vessel-specific mass, the LAD subtended almost half of the LV, followed by the LCX and RCA. The data also reveal that the first septal, diagonal, and OM branches contribute equally to the LV mass.

Median LV mass was 141 grams, similar to previous studies that quantified myocardial mass using other imaging methods or pathology.^{5,14–16} Our analysis showed an inverse correlation between myocardial mass and age, which aligns with previous data showing that myocardial mass rises during adolescence and declines during adulthood.¹⁷ Although advanced age has been associated with LV hypertrophy in some studies, research indicates that aging is also accompanied by increased apoptosis of LV myocytes.¹⁸ This reduction in myocyte number is partially compensated by hypertrophy of the remaining myocytes, leads to a decline in LV mass observed with increasing age. Additionally, age-related changes in extracellular matrix composition and myocardial fibrosis may contribute to

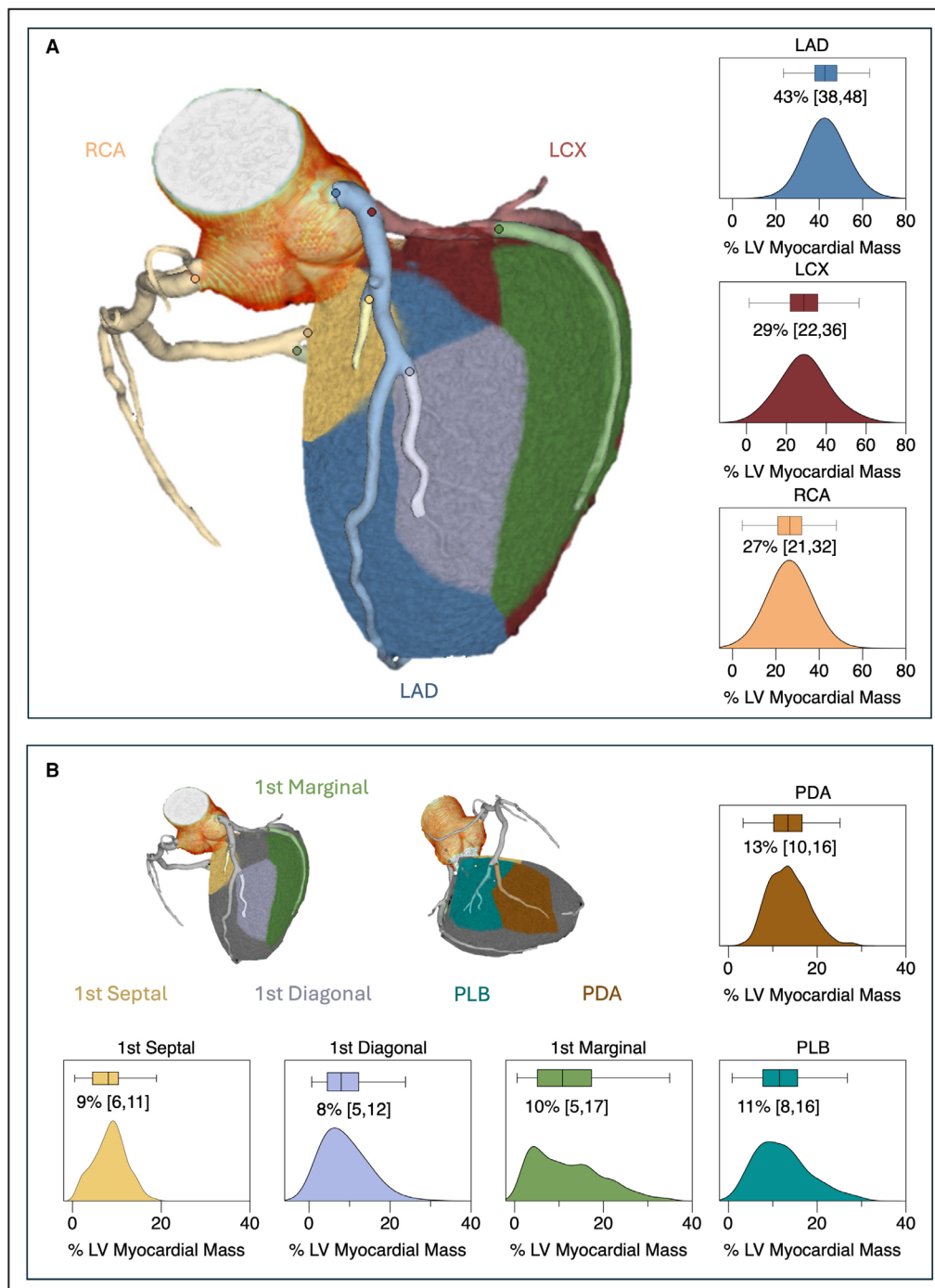


Figure 3. Distribution of vessel-specific myocardial mass with median and interquartile values.

A, Myocardial mass subtended by the main coronary arteries: LAD, LCX, and RCA. **B**, Myocardial mass subtended by coronary artery branches: first septal, first diagonal, first obtuse marginal, PDA, and PLB. LAD indicates left anterior descending; LCX, left circumflex; LV, left ventricular; PCA, posterior descending artery; PLB, posterolateral branch; and RCA, right coronary artery.

this phenomenon.¹⁹ Our data also confirm relationships between LV mass and sex, race, and BMI.²⁰ We observed that women on average had 30% less LV mass than men, in line with Fairbairn et al, who reported that women had approximately 20% less LV mass than

men.²¹ In the multivariable analysis, age, sex, BMI, and hypertension were independently associated with LV mass.

This is the first study to assess the distribution of LV mass subtended by each artery of the coronary

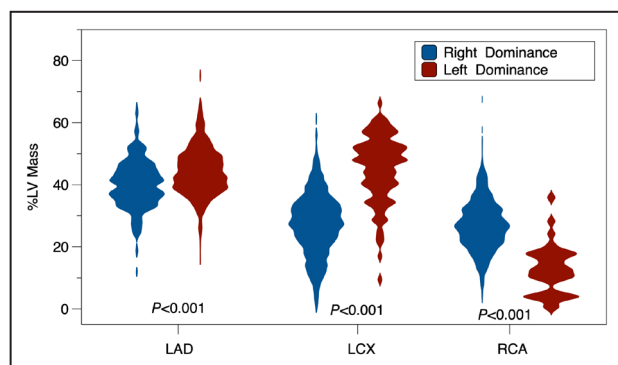


Figure 4. Comparison of LV mass subtended by main coronary vessels based on coronary dominance.

LAD indicates left anterior descending; LCX, left circumflex; LV, left ventricular; and RCA, right coronary artery.

circulation. We report the 5th and 95th percentiles of myocardial mass for all coronary vessels and branches, thereby defining reference ranges for vessel-specific myocardial mass (Table S7). Kim et al estimated vessel-specific myocardial mass using vessel length and allometric scaling for side branches in coronary bifurcations.²² The main difference with the present study is that we measured the mass subtended by each coronary vessel using a fully automated method with CCTA images. Additionally, the population in the present study included both White and Asians. Interestingly, we found that Asian patients have 10% lower myocardial mass and less frequently have a left dominant coronary circulation compared with White patients. This finding aligns with Ihdahid et al who described significant ethnic differences in LV mass.²³

Myocardial mass at risk strongly influences revascularization strategies. Half of all diagonals, marginals, posterior descending, and posterolateral branch branches subtended >10% of the LV mass. Surprisingly, the first septal branch subtends a similar amount of LV mass as the first diagonal and OM branches. These findings have clinical implications. During percutaneous coronary intervention, strategies are implemented to avoid compromising blood flow in significant side branches. Therefore, quantifying myocardial mass at risk during percutaneous coronary intervention planning may lead to tailored strategies aimed at reducing the incidence of side-branch occlusion, potentially minimizing periprocedural myocardial infarction.

Using coronary CT for percutaneous coronary intervention planning has the potential to improve clinical outcomes. Quantifying myocardial mass is a key element in the planning phase of the procedure.²⁴ Currently, the clinical significance of side branches is based on a visual assessment of the vessel size.²⁵ However, visual assessment of the angiogram is limited by foreshortening and overlap, and, like most visual

estimations, is associated with reduced reproducibility and increased interobserver variability. Although a direct comparison between visual and CCTA quantification of myocardial mass has yet to be performed, systematic reporting of mass at risk in patients with CCTA could enhance revascularization by standardizing information about the mass at risk, especially in patients with bifurcation lesions. Additionally, knowledge of the mass at risk may also improve the evaluation of patients with intermediate epicardial lesions, given the relationships among myocardial mass, coronary blood flow, and translesional pressure gradients. Intermediate lesions subtending larger LV territories are more likely to generate pressure gradients than those with the same anatomical lesion severity but subtending smaller mass.

Limitations

The present analysis has several limitations. First, although it represents the largest dataset to date for evaluating vessel-specific myocardial mass, the population included was limited to individuals of Asian and White races, mainly due to the geographic location of the contributing studies. As such, further validation in more diverse populations is warranted. Second, patients included had CAD; thus, these results need to be confirmed in healthy individuals. Additionally, the Voronoi's lacks validation in specific subsets of patients, for example, chronic total occlusion and after myocardial infarction. Further studies should assess the performance of this method in these groups. Moreover, we did not collect information about the angiographic presence of a chronic total occlusion. Third, the software does not account for the right ventricular mass, which could lead to an underestimation of the myocardial mass subtended by the RCA. Finally, this study described the vessel-specific mass; the association of mass quantification using CCTA with outcomes requires further investigation.

CONCLUSIONS

This study used CCTA to quantify the myocardial mass subtended by each epicardial artery of the coronary circulation. Our findings demonstrate that myocardial mass is smaller in older individuals, women, and Asian patients. The LAD was found to subtend nearly half of the LV mass, followed by the LCX and RCA, with the first septal, diagonal, and OM branches contributing equally to the LV mass. Understanding vessel-specific mass at risk has significant clinical implications and holds the potential to enhance the management of patients with CAD. These findings underscore the importance of personalized approaches in assessing and treating CAD.

ARTICLE INFORMATION

Received September 20, 2024; accepted July 17, 2025.

Affiliations

Cardiovascular Center OLV Hospital, Aalst, Belgium (N.S., T.M., F.B., K.I., A.T., D.M., T.M., A.W., K.S., P.A., J.S., B.D.B., C.C.); Department of Clinical Pharmacology, Showa University, Tokyo, Japan (T.M.); Toulouse University Hospital, Toulouse, France (F.B.); Tokyo Medical University, Hachioji Medical Center, Tokyo, Japan (K.I.); Aichi Medical University Hospital, Nagakute, Aichi, Japan (A.T., T.A., H.A.); Department of Clinical and Molecular Medicine, Sapienza University, Rome, Italy (A.W.); Department of Cardiology, St Francis Hospital and Heart Center, Roslyn, New York (K.S.); Department of Medicine, Division of Cardiology, Showa University School of Medicine, Tokyo, Japan (K.S., T.S.); Department of Cardiology, Aarhus University Hospital, Skejby, Aarhus, Denmark (B.N., E.H.C.); Department of Cardiology, Rigshospitalet, Copenhagen University Hospital, Copenhagen, Denmark (T.E.); University of British Columbia, Vancouver, British Columbia, Canada (J.L.); Humanitas Research Hospital IRCCS, Rozzano-Milan, Italy (G.S.); IRCCS Centro Cardiologico Monzino, Milan, Italy (A.B.); Liverpool Heart and Chest Hospital NHS Foundation Trust, Liverpool, UK (T.F.); The Newcastle Upon Tyne Hospitals NHS Foundation Trust, Newcastle, UK (A.B.); Monash Cardiovascular Research Centre, Monash University and Monash Heart; Monash Health, Clayton, Victoria, Australia (B.K.); Weatherhead PET Center; Division of Cardiology, Department of Medicine, McGovern Medical School at UTHealth and Memorial Hermann Hospital, Houston, Texas (N.P.J.); School Cardiovascular and Metabolic Health, University of Glasgow, Glasgow, UK (C.B.); School of Cardiovascular Medicine and Sciences, St Thomas' Hospital Campus, King's College London, London, UK (D.P.); Kobe University, Kobe, Japan (H.O.); Department of Medicine, Seoul National University Hospital, Seoul, Korea (B.K.K.); Department of Cardiology, University of Rome La Sapienza, Rome, Italy (E.B.); Institut d'Investigacions Biomèdiques August Pi i Sunyer (IDIBAPS), university of Barcelona, Barcelona, Spain (S.B.); School Cardiovascular and Metabolic Health, University of Glasgow, NHS Golden Jubilee Hospital, Glasgow, UK (D.C.); Cardiology Unit, Azienda Ospedaliera Universitaria di Ferrara, Ferrara, Italy (G.C.); Lille University Hospital, Lille, France (E.V.B.); Johannes Gutenberg University Mainz, Mainz, Germany (T.G.); Radboud University Nijmegen, Nijmegen, Netherlands (L.V.N.); Institute of Cardiology in Anin, Warsaw, Poland (A.W.); St George's, University of London, London, UK (J.S.); AHEPA University Hospital, Thessaloniki, Greece (G.S.); and Division of University Cardiology, IRCCS Ospedale Galeazzi - Sant'Ambrogio, Milan, Italy (D.A.).

Sources of Funding

None.

Disclosures

Takuya Mizukami reports receiving research grants from Boston Scientific, and speaker fees from Abbott Vascular, CathWorks, and Boston Scientific. Frederic Bouisset received unrestricted grants from the Federation Française de Cardiologie, and consultancy fees from Boston Scientific, B-Braun, Abbott, and Amgen. Daniel Munhoz reports speaker fees from Abbott Vascular. Thomas Engstroem reports speaker and advisory board fees from Abbott, Boston Scientific, and Novo Nordisk. Nils P. Johnson received internal funding from the Weatherhead PET Center for Preventing and Reversing Atherosclerosis; has received significant institutional research support from St. Jude Medical (CONTRAST, NCT02184117) and Philips Volcano (DEFINE-FLOW, NCT02328820) for other studies using intracoronary pressure and flow sensors; has an institutional licensing agreement with Boston Scientific for the smart-minimum fractional flow reserve algorithm (now commercialized under 510(k) K191008); and has patents pending on diagnostic methods for quantifying aortic stenosis and transcatheter aortic valve implantation physiology, and on methods to correct pressure tracings from fluid-filled catheters. Colin Berry receives research funding from the British Heart Foundation (RE/18/6134217, BHF/FS/17/26/32744, PG/19/28/34310) and is employed by the University of Glasgow, which holds consultancy and research agreements for his work with Abbott Vascular, AstraZeneca, Boehringer Ingelheim, Corvoventis Research, GlaxoSmithKline, HeartFlow, Menarini, Novartis, Servier, Siemens Healthcare, and Valo Health. Bernard De Bruyne reports receiving consultancy fees from Boston Scientific and Abbott and research grants from Corvoventis Research, Pie Medical Imaging, CathWorks, Boston Scientific, Siemens, HeartFlow, and Abbott Vascular. Divaka Perera reports research grants from Abbott Vascular and speaker fees from Abbott Vascular, Philips, Abiomed, Medtronic, and Shockwave. Damien Collison

has received consulting fees from Abbott. Gianluca Campo reports research grants from GADA, Abbott Vascular, SMT, and Siemens outside the present work. James Spratt reports receiving research grants from Shockwave medical and speaker fees from Abbott Vascular, Boston Scientific, Rampart Medical, Shockwave Medical, and Medtronic. Tetsuya Amano reports receiving lecture fees from Astellas Pharma, Astra Zeneca, Bayer, Daiichi Sankyo, and Bristol-Myers Squibb. Carlos Collet reports receiving research grants from Biosensors, Corvoventis Research, Medis Medical Imaging, Pie Medical Imaging, CathWorks, Boston Scientific, Siemens, HeartFlow, and Abbott Vascular; and consultancy fees from HeartFlow, OpSens Medical, Abbott Vascular, and Philips Volcano, and has patents pending on diagnostic methods for coronary artery disease. The remaining authors have no disclosures to report.

Supplemental Material

Figures S1–S6

Tables S1–S7

Movie S1

REFERENCES

- Bolognese L, Dellavesa P, Rossi L, Sarasso G, Bongo AS, Scianaro M. Prognostic value of left ventricular mass in uncomplicated acute myocardial infarction and one-vessel coronary artery disease. *Am J Cardiol*. 1994;73:1–5. doi: [10.1016/0002-9149\(94\)90717-X](https://doi.org/10.1016/0002-9149(94)90717-X)
- de Simone G, Gottdiener JS, Chinali M, Maurer MS. Left ventricular mass predicts heart failure not related to previous myocardial infarction: the Cardiovascular Health Study. *Eur Heart J*. 2008;29:741–747. doi: [10.1093/eurheartj/ehm605](https://doi.org/10.1093/eurheartj/ehm605)
- Laukkanen JA, Khan H, Kurl S, et al. Left ventricular mass and the risk of sudden cardiac death: a population-based study. *J Am Heart Assoc*. 2024;3:e001285. doi: [10.1161/JAHA.114.001285](https://doi.org/10.1161/JAHA.114.001285)
- Hachamovitch R, Hayes SW, Friedman JD, Cohen I, Berman DS. Comparison of the short-term survival benefit associated with revascularization compared with medical therapy in patients with no prior coronary artery disease undergoing stress myocardial perfusion single photon emission computed tomography. *Circulation*. 2003;107:2900–2906. doi: [10.1161/01.CIR.0000072790.23090.41](https://doi.org/10.1161/01.CIR.0000072790.23090.41)
- Devereux RB, Roman MJ. Inter-relationships between hypertension, left ventricular hypertrophy and coronary heart disease. *J Hypertens*. 1993;11(4):S3–S9. doi: [10.1097/00004872-199306003-00003](https://doi.org/10.1097/00004872-199306003-00003)
- Greupner J, Zimmermann E, Grohmann A, et al. Head-to-head comparison of left ventricular function assessment with 64-row computed tomography, biplane left cineventriculography, and both 2- and 3-dimensional transthoracic echocardiography: comparison with magnetic resonance imaging as the reference s. *J Am Coll Cardiol*. 2012;59:1897–1907. doi: [10.1016/j.jacc.2012.01.046](https://doi.org/10.1016/j.jacc.2012.01.046)
- Kurata A, Kono A, Sakamoto T, Kido T, Mochizuki T, Higashino H, Abe M, Coenen A, Saru-Chelu RG, de Feyter PJ, et al. Quantification of the myocardial area at risk using coronary CT angiography and Voronoi algorithm-based myocardial segmentation. *Eur Radiol*. 2015;25:49–57. doi: [10.1007/s00330-014-3388-2](https://doi.org/10.1007/s00330-014-3388-2)
- Keulards DCJ, Fournier S, van't Veer M, et al. Computed tomographic myocardial mass compared with invasive myocardial perfusion measurement. *Heart*. 2020;106:1489–1494. doi: [10.1136/heartjnl-2020-316689](https://doi.org/10.1136/heartjnl-2020-316689)
- Narula J, Chandrashekar Y, Ahmadi A, Abbasa S, Berman DS, Blankstein R, Leipsic J, Newby D, Nicol ED, Nieman K, et al. SCCT 2021 expert consensus document on coronary computed tomographic angiography: a report of the Society of Cardiovascular Computed Tomography. *J Cardiovasc Comput Tomogr*. 2021;15:192–217. doi: [10.1016/j.jcct.2020.11.001](https://doi.org/10.1016/j.jcct.2020.11.001)
- Ide S, Sumitsuiji S, Yamaguchi O, Sakata Y. Cardiac computed tomography-derived myocardial mass at risk using the Voronoi-based segmentation algorithm: a histological validation study. *J Cardiovasc Comput Tomogr*. 2017;11:179–182. doi: [10.1016/j.jcct.2017.04.007](https://doi.org/10.1016/j.jcct.2017.04.007)
- Murai T, van de Hoef TP, van den Boogert TPW, et al. Quantification of myocardial mass subtended by a coronary stenosis using intracoronary physiology. *Circ Cardiovasc Interv*. 2024;12:e007322. doi: [10.1161/CIRCINTERVENTIONS.118.007322](https://doi.org/10.1161/CIRCINTERVENTIONS.118.007322)
- Tanabe Y, Kido T, Kurata A, Uetani T, Kuwahara N, Morikawa T, Kawaguchi N, Kido T, Nishimura K, Ikeda S, et al. Combined assessment of subtended myocardial volume and myocardial blood flow for

- diagnosis of obstructive coronary artery disease using cardiac computed tomography: a feasibility study. *J Cardiol*. 2020;76:259–265. doi: [10.1016/j.jcc.2020.03.006](https://doi.org/10.1016/j.jcc.2020.03.006)
13. Sianos G, Morel MA, Kappetein AP, Morice MC, Colombo A, Dawkins K, van den Brand M, van Dyck N, Russell ME, Mohr FW, et al. The SYNTAX score: an angiographic tool grading the complexity of coronary artery disease. *EuroIntervention*. 2005;1:219–227.
 14. Ogawa R, Takahashi N, Higuchi T, Shibuya H, Yamazaki M, Yoshimura N, Takatsuka H, Aoyama H. Assessment of a simple method of heart weight estimation by postmortem computed tomography. *Forensic Sci Int*. 2019;296:22–27. doi: [10.1016/j.forsciint.2018.12.019](https://doi.org/10.1016/j.forsciint.2018.12.019)
 15. Stolzmann P, Scheffel H, Leschka S, Schertler T, Frauenfelder T, Kaufmann PA, Marincek B, Alkadhi H. Reference values for quantitative left ventricular and left atrial measurements in cardiac computed tomography. *Eur Radiol*. 2008;18:1625–1634. doi: [10.1007/s00330-008-0939-4](https://doi.org/10.1007/s00330-008-0939-4)
 16. Gheorghe AG, Fuchs A, Jacobsen C, et al. Cardiac left ventricular myocardial tissue density, evaluated by computed tomography and autopsy. *BMC Med Imaging*. 2019;19:15–22. doi: [10.1186/s12880-019-0326-4](https://doi.org/10.1186/s12880-019-0326-4)
 17. Cain PA, Ahl R, Hedstrom E, Ugander M, Allansdotter-Johnsson A, Friberg P, Marild S, Arheden H. Physiological determinants of the variation in left ventricular mass from early adolescence to late adulthood in healthy subjects. *Clin Physiol Funct Imaging*. 2005;25:332–339. doi: [10.1111/j.1475-097X.2005.00632.x](https://doi.org/10.1111/j.1475-097X.2005.00632.x)
 18. Kurogi K, Ishii M, Nagatomo T, Tokai T, Kaichi R, Takae M, Mori T, Komaki S, Yamamoto N, Tsujita K. Mean density of computed tomography for predicting rotational atherectomy during percutaneous coronary intervention. *J Cardiovasc Comput Tomogr*. 2023;17:120–129. doi: [10.1016/j.jcct.2023.02.002](https://doi.org/10.1016/j.jcct.2023.02.002)
 19. Olivetti G, Melissari M, Capasso JM, Anversa P. Cardiomyopathy of the aging human heart. Myocyte loss and reactive cellular hypertrophy. *Circ Res*. 1991;68:1560–1568. doi: [10.1161/01.res.68.6.1560](https://doi.org/10.1161/01.res.68.6.1560)
 20. Cheng S, Fernandes VRS, Bluemke DA, McClelland RL, Kronmal RA, Lima JAC. Age-related left ventricular remodeling and associated risk for cardiovascular outcomes: the Multi-Ethnic Study of Atherosclerosis. *Circ Cardiovasc Imaging*. 2009;2:191–198. doi: [10.1161/CIRCIMAGING.108.819938](https://doi.org/10.1161/CIRCIMAGING.108.819938)
 21. Fairbairn TA, Dobson R, Hurwitz-Koweek L, Matsuo H, Norgaard BL, Rønnow Sand NP, Nieman K, Bax JJ, Pontone G, Raff G, et al. Sex differences in coronary computed tomography angiography-derived fractional flow reserve: lessons from ADVANCE. *J Am Coll Cardiol Img*. 2020;13:2576–2587. doi: [10.1016/j.jcmg.2020.07.008](https://doi.org/10.1016/j.jcmg.2020.07.008)
 22. Kim HY, Doh JH, Lim HS, Nam CW, Shin ES, Koo BK, Lee JM, Park TK, Yang JH, Song YB, et al. Identification of coronary artery side branch supplying myocardial mass that may benefit from revascularization. *JACC Cardiovasc Interv*. 2017;10:571–581. doi: [10.1016/j.jcin.2016.11.033](https://doi.org/10.1016/j.jcin.2016.11.033)
 23. Ildayhid AR, Fairbairn TA, Gulsin GS, Tzimas G, Danehy E, Updegrove A, Jensen JM, Taylor CA, Bax JJ, Sellers SL, et al. Cardiac computed tomography-derived coronary artery volume to myocardial mass. *J Cardiovasc Comput Tomogr*. 2022;16:198–206. doi: [10.1016/j.jcct.2021.10.007](https://doi.org/10.1016/j.jcct.2021.10.007)
 24. Bouisset F, Ohashi H, Andreini D, Collet C. Role of coronary computed tomography angiography to optimise percutaneous coronary intervention outcomes. *Heart*. 2024;110:1056–1062. doi: [10.1136/heartjnl-2023-322889](https://doi.org/10.1136/heartjnl-2023-322889)
 25. Lee HS, Kim U, Yang S, Murasato Y, Louvard Y, Song YB, Kubo T, Johnson TW, Hong SJ, Omori H, et al. Physiological approach for coronary artery bifurcation disease: position statement by Korean, Japanese, and European bifurcation clubs. *JACC Cardiovasc Interv*. 2022;15:1297–1309. doi: [10.1016/j.jcin.2022.05.002](https://doi.org/10.1016/j.jcin.2022.05.002)